

SCD1 activity promotes cell migration via a PLD-mTOR pathway in the MDA-MB-231 triple-negative breast cancer cell line

Marine Lingrand, Simon Lalonde, Antoine Jutras-Carignan, Karl-F. Bergeron, Eric Rassart and Catherine Mounier*

Molecular Metabolism of Lipids Laboratory, Biological Sciences Department, University of Quebec in Montreal (UQAM)

* **To whom correspondence should be addressed:** Catherine Mounier, Biological Sciences Department, UQAM, 141 President-Kennedy Avenue, Montreal (Quebec), Canada H2X 1Y4, 1-514-897-3000 extension 8912, mounier.catherine@uqam.ca

Author contributions: KFB and CM designed the project. ML, SL and AJC performed experiments. ML and KFB wrote the manuscript. KFB, ER and CM edited the manuscript.

Word count: 7 326

Number of Figures: 8

Number of Tables: none

Quantity of supplemental data: 1 supplementary figure

Abstract

Background

Breast cancer is the most common cancer in women. Despite high survival rates in Western countries, treatments are less effective in metastatic cases and triple-negative breast cancer (TNBC) patient survival is the shortest across breast cancer subtypes. High expression levels of stearoyl-CoA desaturase-1 (*SCD1*) have been reported in breast cancer. The SCD1 enzyme catalyzes the formation of oleic acid (OA), a lipid stimulating the migration of metastatic breast cancer cells. Phospholipase activity is also implicated in breast cancer metastasis, notably phospholipase D (PLD).

Methods

Kaplan-Meier survival plots generated from gene expression databases were used to analyze the involvement of *SCD1* and *PLD* in several cancer subtypes. SCD1 enzymatic activity was modulated with a pharmaceutical inhibitor or by OA treatment (to mimic SCD1 over-activity) in three breast cancer cell lines: TNBC-derived MDA-MB-231 cells as well as non-TNBC MCF-7 and T47D cells. Cell morphology and migration properties were characterized by various complementary methods.

Results

Our survival analyses suggest that *SCD1* and *PLD2* expression in the primary tumor are both associated to metastasis-related morbid outcomes in breast cancer patients. We show that modulation of SCD1 activity is associated with the modification of TNBC cell migration properties, including changes in speed, direction and cell morphology. Cell migration properties are regulated by SCD1 activity through a PLD-mTOR/p70S6K signaling pathway. These effects are not observed in non-TNBC cell lines.

Conclusion

Our results establish a key role for the lipid desaturase SCD1 and delineate an OA-PLD-mTOR/p70S6K signaling pathway in TNBC-derived MDA-MB-231 cell migration.

Abbreviations:

mTOR: mammalian target of rapamycin; SCD1: stearoyl-coenzyme A desaturase-1; OA: oleic acid; POA: palmitoleic acid; PLD: phospholipase D; p70S6K: p70S6 kinase; TNBC: triple-negative breast cancer; BSA: bovine serum albumin; DMSO: dimethyl sulfoxide

Keywords: stearoyl-coenzyme A desaturase-1; oleic acid; phospholipase D; mammalian target of rapamycin; triple-negative breast cancer

Introduction

Breast cancers are classified into different subtypes according to the presence or absence of key molecular markers. Triple-negative breast cancer (TNBC) patient survival is the shortest across breast cancer subtypes [1]. TNBC is characterized by the lack of estrogen and progesterone receptors as well as human epidermal growth factor receptor-2 amplification [2]. TNBC is aggressive, invasive and highly metastatic, rendering it particularly difficult to treat. Metastasis, a multistep process leading to cancer dissemination from the primary tumor, involves several complex cell behaviors including epithelial-mesenchymal transition, intra/extravasation, migration and proliferation [3, 4].

Stearoyl-coenzyme A desaturase-1 (SCD1) catalyzes the $\Delta 9$ -desaturation of saturated fatty acids to produce mono-unsaturated fatty acids: oleic acid (OA) and palmitoleic acid (POA). Changes in saturated and mono-unsaturated fatty acid levels can alter a wide range of cellular mechanisms involved in carcinogenesis, such as membrane phospholipid synthesis, energy metabolism, and inflammation signaling [5, 6]. Interestingly, lipid desaturation has also been correlated with higher breast cancer risk [7, 8]. Previous studies have established a key role for SCD1 in several types of human cancers such as prostate, colon, kidney, liver, lung and even breast cancer [9-14]. SCD1 is thought to be an important factor in cell proliferation by regulating anti-apoptosis signals, which would promote cell growth and survival [9, 15]. Moreover, SCD1 has been associated to a metabolism state favoring tumor growth [5, 9, 16]. High levels of *SCD1* expression have previously been associated with breast cancer [14, 17]. However, these studies have mainly focused on the development of the primary breast tumor. A possible role for SCD1 in the metastatic process has only begun to be explored. Elevated *SCD1* expression has interestingly been reported in breast tumors with increased probability of metastatic progression [18]. Moreover, our group has previously shown that SCD1 plays a role in the epithelial-mesenchymal transition of breast cancer cells in culture [19], thereby hinting at a possible role for SCD1 in the metastatic process.

OA, the main product of SCD1 activity, has been shown to promote TNBC-derived MDA-MB-231 cell migration by a phospholipase C-dependent mechanism [20]. In addition, OA induces MDA-MB-231 cell proliferation by activating G protein-coupled receptor 40 [21, 22]. Phosphatidic acids, a family of labile signaling lipids produced by phospholipase D (PLD) activity, also stimulate TNBC cell migration and invasion [23, 24]. In a breast tumor xenograft model, tumor growth and metastasis are stimulated following phosphatidic acid overproduction [25]. Interestingly, the PLD2 enzyme isoform can be selectively activated by unsaturated fatty acids like OA [26-28]. PLD activity, particularly of the PLD2 isoenzyme, stimulates cancer cell migration [24, 29]. Moreover, PLD activity is known to be regulated by cell surface receptors: G protein-coupled receptors and receptor tyrosine kinases [28]. Therefore, the possibility of a conjunct role of SCD1 and PLD in breast tumorigenesis, particularly the PLD2 isoenzyme, warrants exploration.

In the present study, we confirm that migration of the TNBC-derived MDA-MB-231 cell line is most responsive to OA compared to non-TNBC cell lines. PLD activity appears necessary for the effect of OA on MDA-MB-231 cell migration speed. Corresponding changes in cell morphology are associated with the modification of MDA-MB-231 cell

migration properties following OA-treatment: cells are more elongated and undergo less directional changes during migration. Taken together, our results underline the key role of SCD1 activity, and delineate an OA-PLD-mTOR/p70S6K signaling pathway, in TNBC-derived MDA-MB-231 cell migration.

Material and Methods

Kaplan-Meier plots

The breast cancer Kaplan-Meier plotter (kmplot.com) [30] was used to generate distant metastasis-free survival plots over a period extending up to 180 months. Patients were separated into two groups according to expression values for *SCD1* (Affymetrix probe ID 200832_s_at), *PLD1* (probe 177_at) or *PLD2* (probe 209643_s_at) in their primary tumor using the 'best cutoff' option. All breast cancers (n=1747) and triple-negative breast cancers (n=43) were considered. To evaluate differences between groups, statistical analyses using the log-rank test as well as the proportional hazards model were made.

Datasets included in analysis: E-MTAB-365, E-TABM-43, GSE11121, GSE12093, GSE12276, GSE1456, GSE16391, GSE16446, GSE16716, GSE17705, GSE17907, GSE18728, GSE19615, GSE20194, GSE20271, GSE2034, GSE20685, GSE20711, GSE21653, GSE2603, GSE26971, GSE2990, GSE31448, GSE31519, GSE32646, GSE3494, GSE37946, GSE41998, GSE42568, GSE45255, GSE4611, GSE5327, GSE6532, GSE7390, GSE9195.

Cell culture and treatments

MCF-7 and T47D breast cancer cells (gifts from Dr J. J. Lebrun, McGill University), as well as MDA-MB-231 breast cancer cells (MDA-MB-231-luc-D3H2LN; PerkinElmer, #119369) were grown in complete Eagle's minimum essential medium (EMEM) media (Wisent, #320-005-CL) supplemented with 10% fetal bovine serum (FBS), 500 U/mL penicillin and 500 µg/mL streptomycin (LT Gibco, #15070063). Cells were maintained in a 5% CO₂ incubator at 37°C up to a maximum of 25 passages. All treatments were performed in serum-free EMEM media. Stocks of bovine serum albumin (BSA)-conjugated fatty acids were prepared at a 2:1 molar ratio (3.33mM fatty acid: 1.7mM BSA). Treatments with 50 µM oleic acid (OA; Sigma, #O-3008) and palmitoleic acid (POA; Cayman chemical company, #10009871) were performed for 24h using BSA as vehicle and control. Treatments with 1 µM SCD1 inhibitor (SCD1i) A939572 (Biofine International, #37062) or 10 µM pan-PLD inhibitor (PLDi) VU0285655-1 (Avanti Polar Lipids, #857372) were performed for 4h while treatment with 200 nM rapamycin (Calbiochem EMD Biosciences, #53123-88-9) was performed for 24h using dimethyl sulfoxide (DMSO) as vehicle.

Kinetic wound healing assay

MCF-7, T47D and MDA-MB-231 cells were seeded in 24-well plates at a density of 5x10⁴ cells per well. The next day, cells were treated for 24h with fatty acids (OA, POA) and rapamycin. Cells were treated with SCD1i, PLDi or a combination of both inhibitors during the last 4h of the 24h treatment period. The confluent cell monolayer was scratched, and wound recovery was monitored under 5% CO₂ and at 37°C. During this

12h live imaging period, images were acquired every 15 min using a Nikon Eclipse Ti inverted microscope. Wound area at each acquisition was measured using NIS-Elements software (Nikon). Wound recovery corresponds to the shrinking wound surface relative to the initial area. Individual cells (30 cells per treatment condition) were tracked with ImageJ software to determine cell migration speed and average distance between each acquisition step. The directionality ratio is the distance between initial and end point divided by the total migration path length. Cell trajectory tracings and vector diagrams were generated with ImageJ software.

Cell morphology

MDA-MB-231 cells were seeded at a density of 1×10^4 cells per well (60-70% confluency) and grown on coverslips. Cells were then fixed with 4% paraformaldehyde and nuclei were stained with 4',6-diamidino-2-phenylindole (DAPI) while actin filaments were stained with Phalloidin-Alexa 488 (Cytoskeleton, #PHDG1-A). Images were captured through the cell nuclei (single confocal slice) using a Nikon Eclipse Ti inverted microscope. Three independent experiments were performed with ~40 cells analyzed per experiment and per treatment condition. Area, perimeter and Ferret diameter (largest possible cell diameter) were measured with ImageJ software. The roundness index ($\text{perimeter}^2/4*\pi*\text{area}$) is a value from 0 to 1, where 1 symbolizes a perfect circle.

Protein extraction and Western blotting

MDA-MB-231 cells were lysed in RIPA buffer (50 mM Tris-HCl, pH 7.4; 1% NP-40; 0.5% Na-deoxycholate; 0.1% SDS; 150 mM NaCl; 2 mM EDTA; 50 mM NaF) containing protease and phosphatase inhibitors (Sigma, #P8340; #P0044). After centrifugation, proteins were recovered in the supernatant. Protein concentration was determined by the Bradford protein assay (Bio-Rad, #5000006). Proteins were separated on SDS-PAGE transferred to PVDF membranes. Primary antibodies: phospho-mTOR Ser2448 (1:1000; Cell Signaling, #2971), phospho-p70S6K Thr389 (1:1000; Cell Signaling, #9205), mTOR (1:1000; Cell Signaling, #2972S), p70S6K (1:1000; Cell Signaling, #9202), phospho-Akt Ser473 (1:1000; Cell Signaling, #9271), SCD1 (1:1000; Abcam, #ab19862) or α -Tubulin (1 $\mu\text{g}/\text{ml}$; Abcam, #ab4074), were used. HRP-conjugated anti-mouse IgG (1:1000; Cell Signaling, #7076S) and anti-rabbit IgG (1:4000 Cell Signaling, #7074) were used as secondary antibodies. Signals were revealed using the ECL substrate (Millipore, #WBKLS0100). In order to normalize and verify proteins amounts equality, membranes were finally stained with amido black solution (0.25% amido black, 45% MeOH, 45% ddH₂O, 10% glacial HOAc) and de-stained with the same solution without dye.

Foci forming assay

MDA-MB-231 cells were seeded at a density of 1×10^4 cells per well and treated 48h with SCD1i, PLDi or a combination of both inhibitors. After treatment, cells were grown in inhibitor-free EMEM media (detailed above) for up to 7 days in a 5% CO₂ incubator at 37°C to allow for large colonies to form. The colonies were fixed in ice-cold 100% methanol and stained with 0.2% crystal violet in a methanol-water (25:75) solution. Images (36 fields per condition) were acquired with a Nikon Eclipse Ti inverted microscope.

Cell viability assay

MDA-MB-231 cell viability was evaluated with a MTT formazan colorimetric assay (Sigma, #M2003). Cells were seeded at a density of 1.5×10^4 cells per well in EMEM media (detailed above). The next day, cells were treated with SCD1i, PLDi or a combination of both inhibitors for 96h. Cells were transferred to fresh media containing 1 mM MTT and placed in a 5% CO₂ incubator at 37°C for 4h. The formazan crystals were dissolved in lysis solution (10% SDS, 10mM HCl) overnight at 37°C and absorbance was measured at 570 nm with correction at 690 nm with BioTek Eon Microplate Spectrophotometer. MTT concentration is indicative of mitochondrial activity and, by extension, cell viability.

Transwell cell migration and invasion assays

MDA-MB-231 cells were seeded at a density of 5×10^4 cells per well. The next day, cells were treated 4h with SCD1i, PLDi or a combination of both inhibitors. Cells were trypsinized and transferred to a non-coated (migration) or Matrigel-coated (invasion) 8µm pore polycarbonate membrane insert (Corning, #3422) in serum-free EMEM media containing SCD1i, PLDi or a combination of both inhibitors. EMEM media supplemented with 10% FBS was used as a chemoattractant in the bottom part of the chamber. Cells were allowed to migrate through the semi-permeable membrane for 6h. For invasion assays, cells were allowed to migrate through the Matrigel (and semi-permeable membrane) for 24h. Cells were fixed in 4% formaldehyde and nuclei stained with DAPI and counted with ImageJ. Images of the cells located on both sides of the semi-permeable membranes were acquired with a Nikon Eclipse Ti inverted microscope. Images were superposed and cells were counted with ImageJ software (~2000 cells per treatment condition).

Statistical analysis

Unless specified otherwise, data are presented as mean \pm standard error of the mean (SEM). A one-way ANOVA followed by a post hoc Tukey's test was used in order to compare multiple groups at a time. A Student's t-test was used to compare two groups at a time. Generally, a one-tailed unpaired test was applied, except with data normalized to control where a "one sample" t-test was used. A p-value < 0.05 was considered statistically significant. Each independent experiment was completed with distinct cell cultures prepared on different days (independent replicates).

Results

SCD1 expression is associated with morbid outcomes in metastatic breast cancer patients

To evaluate the potential role of *SCD1* expression in metastatic breast cancer, we generated Kaplan-Meier plots of distant metastasis-free survival (DMFS) for breast cancer patients over a period extending up to 180 months using available gene expression dataset records [30]. These informatics analyses reveal that high *SCD1* expression in the primary tumor is significantly associated with an increased proportion of metastasis-related deaths in patients suffering from breast cancers (Fig.1). This association appears

even stronger in TNBC, as reflected by the elevated hazard ratio associated with this cancer subtype (6.73 hazard ratio compared to 1.28 for all breast cancers). Overall, our DMFS analyses support a role for *SCD1* in breast cancer metastasis.

Oleic acid specifically stimulates triple-negative breast cancer cell migration

OA, a product of SCD1 enzymatic activity, is known to stimulate the migration of MDA-MB-231 breast cancer cells [20, 31]. To further characterize the impact of SCD1 activity on breast cancer cell migration, we performed wound healing assays in the presence of the two SCD1 products, OA and POA, to effectively mimic enzymatic over-activity (Fig.2A). We tested three breast cancer cell lines, all derived from metastatic sites: MCF-7, T47D and the TNBC-derived MDA-MB-231. OA specifically increases wound recovery by 1.5 fold in these breast cancer cell lines, while POA has no effect (Fig.2D-F). Notably, both basal and OA-stimulated wound healing amplitudes are more than 4 times higher in the TNBC-derived MDA-MB-231 line (basal: 39%, treated: 59%) relative to the non-TNBC cell lines MCF-7 and T47D (basal: 8 to 9%, treated: 12 to 13%). Since wound healing in our assays could be due to a combination of cell migration and cell proliferation, and given that OA is known to stimulate breast cancer cell proliferation [22], we determined the specific contribution of cell migration to our assays by analyzing individual cell tracks. OA-stimulated cell migration is only observed in the TNBC MDA-MB-231 line (Fig.2B,C). Wound healing in other OA-stimulated cell lines is due to cell proliferation as basal and stimulated migration speeds (as well as distances travelled between each image acquisition) are similar in the non-TNBC MCF-7 and T47D lines (Fig.2B,C). Considering that MDA-MB-231 cells were the only ones whose migration was responsive to OA, we focused our investigation on this TNBC line.

To better understand the effect of OA treatment on MDA-MB-231 cell migration, we further analyzed individual cell tracks in our wound healing assays (Fig.3A). OA increases the migration speed of individual cells (Fig.3C) as reflected by an increase in the distance travelled between each microscope image acquisition (Fig.3D). Intriguingly, the direction of cell migration is deregulated by OA treatment: while control and POA-treated cells typically adopt an overall migration pattern perpendicular to the wound (as determined from the final cell position relative to the initial position, i.e. the cell displacement), most OA-treated cells tend instead to migrate diagonally relative to the wound (Fig.3B). Moreover, OA treatment steadies the direction of cell migration by diminishing the frequency of directional changes, leading to a significant increase in the directionality ratio of MDA-MB-231 cell migration (Fig.3E). To evaluate the importance of SCD1 enzymatic activity in this migration process, we performed transwell chemotaxis assays (migration through a membrane, and invasion through extracellular matrix + membrane) in the presence of A939572, a specific pharmacological inhibitor of SCD1 activity [31, 32]. In both assays, OA strongly stimulates migration while POA has no effect (Fig.4). Interestingly, while the SCD1 inhibitor diminishes transwell migration of unstimulated cells, it has no effect in the presence of OA.

Modulation of SCD1 activity alters MDA-MB-231 cell morphology

Cancer cell morphology can be an indicator of migration behavior [33]. To better understand how SCD1 can modulate TNBC cell migration, we analyzed the morphology of MDA-MB-231 cells following treatment with POA, OA or the SCD1 inhibitor

(Fig.5A). Compared to untreated control cells, OA specifically increases the cell surface area and expands the cell perimeter, while POA has no effect (Fig.5B,C). Cells treated with the SCD1 inhibitor are rounded (less elongated) relative to control. Irrespective of the presence of the SCD1 inhibitor, OA-treated cells adopt a more elongated morphology as reflected by a longer maximum cell diameter (Feret diameter) and a diminished roundness index (Fig.5D,E). These cell shape changes are consistent with the modification of migration properties observed in OA-stimulated cell migration (Fig.3), as elongated cells typically display diminished directional changes and increased migration speed [34].

Oleic acid stimulates MDA-MB-231 migration through a PLD-mTOR/p70S6K pathway

PLD activity, particularly of the PLD2 isoenzyme, has been implicated in the breast cancer metastatic process [25]. OA stimulates the enzymatic activity of the PLD2 isoform, but not the PLD1 isoform [26, 27]. Moreover, *PLD1* expression cannot be significantly associated with metastatic breast cancer patient outcomes via Kaplan-Meier DMFS survival analyses (Fig.6A,B). Intriguingly, high *PLD2* expression in the primary tumor is associated with better patient outcomes when all breast cancers are combined (Fig.6C). Yet *PLD2* expression is also associated with an increased proportion of metastasis-related deaths among TNBC patients (Fig.6D), similarly to what we show for *SCD1* expression above (see Fig.1B).

Phosphatidic acids produced by PLD enzymes can activate and stabilize mTOR complexes [35, 36], which have been shown to play an important role in TNBC progression [37]. To determine if OA-stimulated TNBC cell migration is dependent on mTOR and/or PLD activation, we performed wound healing assays in the presence of specific inhibitors. Indeed, both Rapamycin (a mTOR inhibitor) and VU0285655-1 (a pan-PLD inhibitor with highest specificity for the PLD2 isoenzyme [38, 39]) block the stimulating effect of OA on wound healing and even diminish wound recovery below the unstimulated control level (Fig.6E). We next sought to determine if mTOR activity in OA-stimulated TNBC cells is involved downstream of PLD. Activating phosphorylation of mTOR (Ser2448) and its effector p70S6K (Thr389) in OA-treated MDA-MB-231 cells is blocked by the PLD inhibitor (Fig.6F,G), showing that OA stimulates mTOR/p70S6K signaling via PLD activity.

MDA-MB-231 cell migration is dependent on SCD1 and PLD activity

To further evaluate the role of SCD1 in TNBC cell migration, we determined the impact of SCD1 activity inhibition in several migration assays, alone and in combination with PLD activity inhibition. Treatments with the SCD1 inhibitor reduce wound healing more severely than PLD activity inhibition alone (Fig.7A), suggesting again that SCD1 activity is necessary for the contribution of PLD activity to our assays. In transwell migration and invasion assays however, the lowering effect of SCD1 and PLD inhibitors, both individually and in combination, on MDA-MB-231 cell behavior is undistinguishable (Fig.7B,C), suggesting that SCD1 and PLD act in the same pathway regulating cell migration. Anti-proliferation effects, of the SCD1 inhibitor in particular, might account for the discrepancy observed between our wound healing and cell migration assays, as cell proliferation contributes in part to wound healing. Therefore, we next ascertained the effect of these inhibitors on MDA-MB-231 cell proliferation. Though treatment with each

inhibitor alone tends to diminish the number of foci (a measure of cell proliferation), only co-inhibition of SCD1 and PLD activities clearly diminishes both MDA-MB-231 cell proliferation and cell viability (Fig.7D,E). Altogether, our inhibitor treatment experiment results are consistent with a pathway where SCD1 acts upstream of PLD to regulate cell migration.

Discussion

In this study, we probe the role of SCD1 activity in breast cancer cell migration. An interrelationship between *SCD1* expression, tumor grade and invasive histological classification was previously suggested in breast cancer tissue [8]. Promotion of *SCD1* expression by growth factor signaling has also been associated with migration in breast cancer cell lines [40]. Our Kaplan-Meier survival analyses confirmed that *SCD1* gene expression is linked to breast cancer metastasis in humans. Indeed, we associated high *SCD1* expression in the primary tumor to poor outcomes implicating metastasis, particularly in TNBC patients (Fig.1). A similar association with TNBC patient survival was found for *PLD* expression levels, particularly for *PLD2*, where high expression was correlated to poor DMFS outcomes for TNBC patients (Fig.6B,D). Intriguingly, high *PLD2* expression in the primary tumor was favorable to survival when all breast cancers were combined (Fig.6C). It would be interesting to determine if specific cancer subtypes (other than TNBC) underline this phenomenon. Migration was specifically increased in TNBC-derived MDA-MB-231 cells following treatment with the SCD1 product OA (Fig.2), justifying a more detailed study on MDA-MB-231 cells. POA (a minor SCD1 product compared to OA [41]) had no effect on breast cancer cell migration. OA evidently has specific effects on migrating cells that POA cannot trigger. Furthermore, OA clearly acts downstream of SCD1 activity as the SCD1 inhibitor has no effect in the presence of OA (Figs.4&5). One possibility is that OA, and not POA, is used to modify proteins regulating migration. Such specificity in the biological effect of OA versus POA has been reported for the activity of some proteins: e.g. the Wnt morphogen [42] and the lipogenic transcription factor SREBP1 [43]. High SCD1 expression (and high enzymatic activity leading to OA overproduction) might be particularly relevant in the primary tumor as the three breast cancer cell lines investigated here, all derived from metastatic sites, shared similar SCD1 protein levels (Supplementary Fig.S1) despite reacting differently to OA in our migration assays.

Tumor cell morphology is related to their aptitude to migrate [34]. Cell detachment from the primary tumor and adoption of a lengthened morphology is preliminary to invasion [44-46]. We previously suggested that SCD1 is implicated in the transformation of MDA-MB-231 cells from an epithelial to a mesenchymal phenotype [19]. Accordingly with a role for SCD1 in breast cancer cell morphology changes contributing to metastasis, we show in this current study that inhibition of SCD1 enzymatic activity induces a rounded, less elongated phenotype in MDA-MB-231 cells (Fig.5). Since SCD1 enzymatic activity is directly correlated, at least in liver tissue [47], to the level of mono-unsaturated fatty acids like OA we used fatty acid treatment to mimic SCD1 over-activity. OA treatment resulted in elongated, spindle-shaped MDA-MB-231 cells (Fig.5). This elongated cell morphology is consistent with the increased speed (Figs.2B,C and

3C,D) and diminished directional changes observed during migration (Fig.3A,B). OA treatment steadied the direction of cell migration (Fig.3E), perhaps by rendering migrating cells less pliable and/or less responsive to extracellular cues [48]. It seems paradoxical that wound recovery was more extensive following OA treatment although cells did not tend to migrate perpendicular to the wound and instead migrated diagonally to it. Presumably, the treated cell's streamlined movement and increased speed more than compensated for their lack of directional variation. Of interest, lysophosphatidic acid, a lipid class whose composition often incorporates OA, has also been reported to diminish the directional variation of migrating MDA-MB-231 cells, but it did not increase migration speed [49]. Further investigations will be required to determine if this contrasting effect on migration speed stems from differential cellular processing of these lipids: OA versus oleoyl lysophosphatidic acid. We also characterized the effect of SCD1 activity on TNBC cell invasion through an extracellular matrix (Matrigel). Consistent with the fact that knockdown of *SCD1* expression diminishes MDA-MB-231 cell invasion [19], inhibition of SCD1 activity also reduced it (Fig.7C). Overall, our results clearly implicate SCD1 activity as a stimulating factor in MDA-MB-231 breast cancer cell motility.

We used the VU0285655-1 compound to inhibit PLD activity. Though this inhibitor has a highest specificity for the PLD2 isoenzyme, at the concentration used (10 μ M) this compound also inhibits PLD1 activity [38, 39]. Therefore, we cannot distinguish between PLD1- and PLD2-mediated effects in our assays. The effects of SCD1 or PLD inhibition were undistinguishable in transwell migration/invasion assays suggesting a common signaling pathway (Fig.7B,C). Yet, in our wound healing assays where there is no experimental chemotaxis gradient, SCD1 inhibition had a stronger impact than PLD inhibition (Fig.7A). Perhaps the impact of SCD1 activity on the direction of cell migration underlies part of this phenomenon. Also, since cell proliferation can be a contributing factor to our wound healing assays, and both SCD1 and PLD are known to contribute to the proliferation of breast cancer cell lines [25, 50-52], we reasoned that anti-proliferation effects from the inhibitors might account for their differential effects on wound healing. We estimated the impact of our inhibitors on cell proliferation with a foci formation assay. Interestingly, both SCD1 and inhibitors tended to diminish foci formation, but this effect only became significant when administered together (Fig.7D). Simultaneous exposure to the two inhibitors appeared to be somewhat cytotoxic, as conjunct SCD1 and PLD inhibition also decreased cell viability (Fig.7E). The diminished MDA-MB-231 proliferation we observed after SCD1/PLD co-inhibition might therefore not be entirely caused by reduced enzymatic activity, but be caused in part by pharmacological cytotoxicity. As conjunct SCD1/PLD activity inhibition diminishes both MDA-MB-231 cell proliferation and migration, it might constitute a promising approach for the control of breast cancer progression *in vivo*.

We aimed to delineate the molecular events underlying the effect of SCD1 activity on MDA-MB-231 cell behavior. The SCD1 product OA can be incorporated into membrane phospholipids that are then processed by PLD to generate phosphatidic acids (Fig.8) [53]. Alternatively, PLD2 can be selectively activated by OA [26, 27]. Therefore, we explored the possibility of a sequential mechanism linking SCD1 and PLD activity. We showed that OA stimulated the migration of MDA-MB-231 cells via PLD and mTOR, suggesting

that mTOR is downstream of PLD (Fig.6E). Furthermore, phosphorylation of mTOR/p70S6K following OA treatment was dependent on PLD activity (Fig.6F,G). The products of PLD activity (phosphatidic acids) presumably activated the mTOR/p70S6K axis [35]. In a manner consistent with this scenario, co-inhibition of SCD1 and PLD was not additive in our MDA-MB-231 migration/invasion assays (Fig.7A-C), suggesting that they act in the same molecular pathway. Though the effect of OA on MDA-MB-231 cell behavior was dependent on PLD activity, and could result from an activation of PLD2 by OA, we cannot exclude the possibility that SCD1 and PLD could also act on TNBC cell migration through parallel pathways, some of which have been suggested. For example, through lipid desaturation, SCD1 could influence cell membrane fluidity and signaling activity [54], which might in turn affect cell migration independently of PLD. OA has also been reported to be involved in other phospholipase-dependent signaling pathways stimulating MDA-MB-231 cell migration. Indeed, pharmacological inhibition of diacylglycerol-generating phospholipase C blocked OA-stimulated scratch wound closure via arachidonic acid production [20]. Interestingly, arachidonic acid and diacylglycerols are metabolites that can be derived from phosphatidic acids. As arachidonic acid has also been shown to promote MDA-MB-231 cell migration [55], these phosphatidic acid metabolites might contribute to the activation of the mTOR/p70S6K axis controlling wound closure in our assays.

Taken together, our results strongly suggest that SCD1, through its OA product, could stimulate TNBC progression by activating cancer cell migration, invasion and proliferation. OA stands out as a major signaling lipid (as POA as no effect) modulating cancer cell migration through a PLD-mTOR complex 1 pathway schematically presented in Figure 8.

Acknowledgements: We thank Denis Flipo (UQAM) for confocal microscopy guidance as well as Ji Min Guo (Harvard Medical School, Boston) for advice and tools with survival analysis through Kaplan-Meier plots. We also thank David Rhainds (Montreal Heart Institute) for critical reading of the manuscript.

Disclosure statement: The authors declare that they have no conflict of interest with the contents of this article.

Figure legends

Figure 1. SCD1 expression is associated with morbid outcomes in metastatic triple-negative breast cancer patients. Distant metastasis-free survival (DMFS) Kaplan-Meier plots of (A) all (Global) breast cancer and (B) triple-negative breast cancer patients. Patients were divided into 2 groups based on the level of *SCD1* expression measured by microarray gene expression profiling of their primary tumor (low expression in light blue; high expression in pink) [30]. Hazard ratios (HR) were calculated with a 95% confidence interval and p-values were expressed as logrank P.

Figure 2. Oleic acid stimulates scratch wound closure in several breast cancer cell lines. Wound recovery after scratch through a monolayer of various breast cancer cell lines was monitored every 15 min during a 12h time course. (A) Representative images of scratch wounds through a monolayer of MDA-MB-231 cells at the beginning (*left panels*) and at the end of the time course (*right panels*). Cells were treated with palmitoleic acid (POA; 50 μ M), oleic acid (OA; 50 μ M) or BSA as control (CTRL). Wound area is highlighted in red. Scale bars = 100 μ m. (B,C) Analysis of individual cell motility after scratch (10 cells per experiment) in three untreated breast cancer cell lines: MCF-7 (n=5 independent replicates), T47D (n=3) and MDA-MB-231 cells (n=4). (B) Average cell speed. (C) Distance travelled by tracked cells between each image acquisition. (D-F) Wound recovery as function of time in (D) MCF-7 (10 individual cells per experiment, n=4 independent replicates), (E) T47D (n=3) and (F) MDA-MB-231 cells (n=7). Results are expressed as percentage of wound recovery relative to the initial wound area. Error bars show the standard error of the mean (SEM). A two-way ANOVA was used to calculate statistical significance; p-values **** <0.0001, ** <0.01, * <0.05, ns = not significant.

Figure 3. Oleic acid increases MDA-MB-231 triple-negative breast cancer cell migration speed and directionality. Analysis of individual MDA-MB-231 cell migration trajectories during wound recovery after scratch (10 cells per experiment, n=3 independent replicates). Cells were treated with palmitoleic acid (POA; 50 μ M), oleic acid (OA; 50 μ M) or BSA as control (CTRL), and monitored every 15 min during a 12h time course. Wound area is highlighted in red. (A) Vector diagrams of cell trajectories from one representative experiment. (B) Frequency of overall cell displacement orientation (Rose plots) relative to the scratch wound. (C) Average cell speed. (D) Distance travelled by tracked cells between each image acquisition. (E) Directionality ratio normalized to vehicle control (increased directionality corresponds to diminished directional changes during migration). A two-way ANOVA was used to calculate statistical significance; p-values ** <0.01, * <0.05.

Figure 4. Oleic acid stimulates MDA-MB-231 triple-negative breast cancer cell migration and invasion. MDA-MB-231 cells were treated with palmitoleic acid (POA; 50 μ M), oleic acid (OA; 50 μ M), SCD1 inhibitor A939572 (SCD1i; 1 μ M) or BSA and DMSO as control (CTRL). Representative images of (A) transwell migration and (B) invasion (through Matrigel) assay results. Nuclei of cells that crossed the semi-permeable membrane (labelled in red) were superposed with nuclei of cells that did not cross the semi-permeable membrane (labelled in green). Scale bar: 100 μ m. The proportion of cells having crossed the membrane relative to vehicle control is presented in the bottom panels

(n=3 independent replicates). A two-tailed unpaired t-test was used to calculate statistical significance; p-values **** <0.0001, ***<0.001, ** <0.01, ns = not significant.

Figure 5. SCD1 activity alters MDA-MB-231 cell morphology. (A) Representative confocal images of MDA-MB-231 cells treated with palmitoleic acid (POA; 50 μ M), oleic acid (OA; 50 μ M), SCD1 inhibitor A939572 (SCD1i; 1 μ M) or BSA and DMSO as control (CTRL). Cell actin filaments are labelled in green. Nuclei are labelled in blue. Scale bar = 50 μ m. Quantification of (B) cell area, (C) cell perimeter, (D) maximum Feret diameter (longest cell diameter), and (E) roundness index (where 1 = perfect circle). Approximately 120 cells were analyzed per treatment condition (~40 cells per condition, n=3 independent replicates). A two-way ANOVA was used to calculate statistical significance; p-values **** <0.0001, * <0.05.

Figure 6. Oleic acid promotes MDA-MB-231 wound recovery via PLD and mTOR activities. Distant metastasis-free survival (DMFS) Kaplan-Meier plots of triple-negative breast cancer patients. Patients were divided into 2 groups based on the level of (A) *PLD1* and (B) *PLD2* expression measured by microarray gene expression profiling of their primary tumor (low expression in light blue; high expression in pink) [30]. Hazard ratios (HR) were calculated with a 95% confidence interval and p-values were expressed as logrank P. (C) Wound recovery of MDA-MB-231 cells treated with oleic acid (OA; 50 μ M), PLD inhibitor VU0285655-1 (PLDi; 10 μ M), mTOR inhibitor rapamycin (200 nM) or BSA and DMSO as control (CTRL). Results are expressed as percentage of wound recovery during time, relative to the initial wound area (n=6 independent replicates). Error bars show the standard error of the mean (SEM). A two-way ANOVA was used to calculate statistical significance. (D,E) Phosphorylation of mTOR (Ser2448) and p70S6K (Thr389) relative to total protein levels in treated MDA-MB-231 cells for 4 independent replicates. Levels were normalized to vehicle control for each independent replicate. Representative Western blots (phospho-protein and total protein) are included for each experiment. Loading controls (Amido black) are also provided. A two-tailed unpaired t-test was used to calculate statistical significance; p-values **** <0.0001, ** <0.01, * <0.05.

Figure 7. MDA-MB-231 cell migration depends on the activity of SCD1 and PLD enzymes. MDA-MB-231 cells were treated with the PLD inhibitor VU0285655-1 (PLDi; 10 μ M), SCD1 inhibitor A939572 (SCD1i; 1 μ M) or DMSO as control (CTRL). (A) Scratch wound recovery as a function of time. Results are expressed as percentage of wound recovery relative to the initial wound area (n=8 independent replicates). Error bars show the standard error of the mean (SEM). Representative images of (B) transwell migration and (C) invasion (through Matrigel) assay results. Nuclei of cells that crossed the semi-permeable membrane (labelled in red) were superposed with nuclei of cells that did not cross the semi-permeable membrane (labelled in green). The proportion of cells having crossed the membrane relative to vehicle control is presented in the bottom panels (n=4 independent replicates). (D) Foci formation and (E) cell viability (MTT reduction assay) relative to DMSO vehicle control (n=4 independent replicates). A two-tailed unpaired t-test was used to calculate statistical significance; p-values: **** <0.0001, *** <0.001, ** <0.01, * <0.05.

Figure 8. Hypothetical model of SCD1 and PLD2 activity in triple-negative breast cancer cell migration. Oleic acid, the main SCD1 product, can specifically activate PLD2. Oleic acid is also incorporated into cell phospholipids. PLD generates phosphatidic acids from phospholipids. Phosphatidic acids then activate the mTOR/p70S6K pathway. In this manner, MDA-MB-231 cell migration can be modulated by a PLD-mTOR/p70S6K signaling pathway.

Supplementary Figure Legends

Supplementary Figure S1. SCD1 protein expression is similar in the three breast cancer cell lines tested. Quantification of SCD1 protein expression in MCF-7, T47D and MDA-MB-231 cell extracts (n=3 independent replicates). A representative Western blot is included. Loading controls (Amido Black) are also provided. A two-tailed unpaired t-test was used to calculate statistical significance; ns = non-significant.

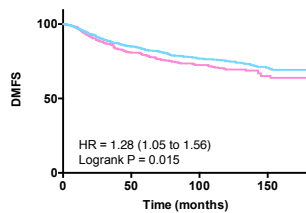
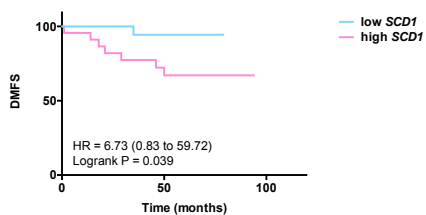
Uncategorized References

1. Kwan, M.L., et al., *Epidemiology of breast cancer subtypes in two prospective cohort studies of breast cancer survivors*. Breast Cancer Res, 2009. **11**(3): p. R31.
2. Hudis, C.A. and L. Gianni, *Triple-negative breast cancer: an unmet medical need*. Oncologist, 2011. **16 Suppl 1**: p. 1-11.
3. Gunasinghe, N.P., et al., *Mesenchymal-epithelial transition (MET) as a mechanism for metastatic colonisation in breast cancer*. Cancer Metastasis Rev, 2012. **31**(3-4): p. 469-78.
4. Saunus, J.M., et al., *Breast Cancer Brain Metastases: Clonal Evolution in Clinical Context*. Int J Mol Sci, 2017. **18**(1).
5. Igal, R.A., *Stearoyl-CoA desaturase-1: a novel key player in the mechanisms of cell proliferation, programmed cell death and transformation to cancer*. Carcinogenesis, 2010. **31**(9): p. 1509-15.
6. Igal, R.A., *Roles of StearoylCoA Desaturase-1 in the Regulation of Cancer Cell Growth, Survival and Tumorigenesis*. Cancers (Basel), 2011. **3**(2): p. 2462-77.
7. Chajes, V., et al., *Fatty-acid composition in serum phospholipids and risk of breast cancer: an incident case-control study in Sweden*. Int J Cancer, 1999. **83**(5): p. 585-90.
8. Guo, S., et al., *Significantly increased monounsaturated lipids relative to polyunsaturated lipids in six types of cancer microenvironment are observed by mass spectrometry imaging*. Sci Rep, 2014. **4**: p. 5959.
9. Mason, P., et al., *SCD1 inhibition causes cancer cell death by depleting mono-unsaturated fatty acids*. PLoS One, 2012. **7**(3): p. e33823.
10. Huang, G.M., et al., *SCD1 negatively regulates autophagy-induced cell death in human hepatocellular carcinoma through inactivation of the AMPK signaling pathway*. Cancer Lett, 2015. **358**(2): p. 180-90.
11. Huang, J., et al., *SCD1 is associated with tumor promotion, late stage and poor survival in lung adenocarcinoma*. Oncotarget, 2016. **7**(26): p. 39970-39979.
12. Fritz, V., et al., *Abrogation of de novo lipogenesis by stearoyl-CoA desaturase 1 inhibition interferes with oncogenic signaling and blocks prostate cancer progression in mice*. Mol Cancer Ther, 2010. **9**(6): p. 1740-54.
13. von Roemeling, C.A., et al., *Stearoyl-CoA desaturase 1 is a novel molecular therapeutic target for clear cell renal cell carcinoma*. Clin Cancer Res, 2013. **19**(9): p. 2368-80.
14. Ide, Y., et al., *Human breast cancer tissues contain abundant phosphatidylcholine(36ratio1) with high stearoyl-CoA desaturase-1 expression*. PLoS One, 2013. **8**(4): p. e61204.
15. Scaglia, N., J.W. Chisholm, and R.A. Igal, *Inhibition of stearoylCoA desaturase-1 inactivates acetyl-CoA carboxylase and impairs proliferation in cancer cells: role of AMPK*. PLoS One, 2009. **4**(8): p. e6812.
16. Nashed, M., J.W. Chisholm, and R.A. Igal, *Stearoyl-CoA desaturase activity modulates the activation of epidermal growth factor receptor in human lung cancer cells*. Exp Biol Med (Maywood), 2012. **237**(9): p. 1007-17.
17. Holder, A.M., et al., *High stearoyl-CoA desaturase 1 expression is associated with shorter survival in breast cancer patients*. Breast Cancer Res Treat, 2013. **137**(1): p. 319-27.

18. Peck, B., et al., *Inhibition of fatty acid desaturation is detrimental to cancer cell survival in metabolically compromised environments*. *Cancer Metab*, 2016. **4**: p. 6.
19. Mauvoisin, D., et al., *Decreasing stearoyl-CoA desaturase-1 expression inhibits beta-catenin signaling in breast cancer cells*. *Cancer Sci*, 2013. **104**(1): p. 36-42.
20. Navarro-Tito, N., et al., *Oleic acid promotes migration on MDA-MB-231 breast cancer cells through an arachidonic acid-dependent pathway*. *Int J Biochem Cell Biol*, 2010. **42**(2): p. 306-17.
21. Soto-Guzman, A., et al., *Oleic acid induces ERK1/2 activation and AP-1 DNA binding activity through a mechanism involving Src kinase and EGFR transactivation in breast cancer cells*. *Mol Cell Endocrinol*, 2008. **294**(1-2): p. 81-91.
22. Hardy, S., et al., *Oleate promotes the proliferation of breast cancer cells via the G protein-coupled receptor GPR40*. *J Biol Chem*, 2005. **280**(14): p. 13285-91.
23. Sliva, D., et al., *Enhancement of the migration of metastatic human breast cancer cells by phosphatidic acid*. *Biochem Biophys Res Commun*, 2000. **268**(2): p. 471-9.
24. Zheng, Y., et al., *Phospholipase D couples survival and migration signals in stress response of human cancer cells*. *J Biol Chem*, 2006. **281**(23): p. 15862-8.
25. Henkels, K.M., et al., *Phospholipase D (PLD) drives cell invasion, tumor growth and metastasis in a human breast cancer xenograph model*. *Oncogene*, 2013. **32**(49): p. 5551-62.
26. Sarri, E., et al., *Endogenous phospholipase D2 localizes to the plasma membrane of RBL-2H3 mast cells and can be distinguished from ADP ribosylation factor-stimulated phospholipase D1 activity by its specific sensitivity to oleic acid*. *Biochem J*, 2003. **369**(Pt 2): p. 319-29.
27. Kim, J.H., et al., *Selective activation of phospholipase D2 by unsaturated fatty acid*. *FEBS Lett*, 1999. **454**(1-2): p. 42-6.
28. Bruntz, R.C., C.W. Lindsley, and H.A. Brown, *Phospholipase D signaling pathways and phosphatidic acid as therapeutic targets in cancer*. *Pharmacol Rev.*, 2014. **66**(4): p. 1033-79. doi: 10.1124/pr.114.009217.
29. Knoepp, S.M., et al., *Effects of active and inactive phospholipase D2 on signal transduction, adhesion, migration, invasion, and metastasis in EL4 lymphoma cells*. *Mol Pharmacol*, 2008. **74**(3): p. 574-84.
30. Gyorffy, B., et al., *An online survival analysis tool to rapidly assess the effect of 22,277 genes on breast cancer prognosis using microarray data of 1,809 patients*. *Breast Cancer Res Treat*, 2010. **123**(3): p. 725-31.
31. Angelucci, C., et al., *Pivotal role of human stearoyl-CoA desaturases (SCD1 and 5) in breast cancer progression: oleic acid-based effect of SCD1 on cell migration and a novel pro-cell survival role for SCD5*. *Oncotarget*, 2018. **9**(36): p. 24364-24380.
32. Tracz-Gaszewska, Z. and P. Dobrzyn, *Stearoyl-CoA Desaturase 1 as a Therapeutic Target for the Treatment of Cancer*. *Cancers (Basel)*, 2019. **11**(7).
33. Clark, A.G. and D.M. Vignjevic, *Modes of cancer cell invasion and the role of the microenvironment*. *Curr Opin Cell Biol*, 2015. **36**: p. 13-22.

34. Petrie, R.J., A.D. Doyle, and K.M. Yamada, *Random versus directionally persistent cell migration*. Nat Rev Mol Cell Biol, 2009. **10**(8): p. 538-49.
35. Foster, D.A., *Phosphatidic acid signaling to mTOR: signals for the survival of human cancer cells*. Biochim Biophys Acta, 2009. **1791**(9): p. 949-55.
36. Toschi, A., et al., *Regulation of mTORC1 and mTORC2 complex assembly by phosphatidic acid: competition with rapamycin*. Mol Cell Biol, 2009. **29**(6): p. 1411-20.
37. Costa, R.L.B., H.S. Han, and W.J. Gradishar, *Targeting the PI3K/AKT/mTOR pathway in triple-negative breast cancer: a review*. Breast Cancer Res Treat, 2018. **169**(3): p. 397-406.
38. Lavieri, R., et al., *Design and synthesis of isoform-selective phospholipase D (PLD) inhibitors. Part II. Identification of the 1,3,8-triazaspiro[4,5]decan-4-one privileged structure that engenders PLD2 selectivity*. Bioorg Med Chem Lett, 2009. **19**(8): p. 2240-3.
39. Cheol Son, J., et al., *Phospholipase D inhibitor enhances radiosensitivity of breast cancer cells*. Exp Mol Med, 2013. **45**: p. e38.
40. Angelucci, C., et al., *Stearoyl-CoA desaturase 1 and paracrine diffusible signals have a major role in the promotion of breast cancer cell migration induced by cancer-associated fibroblasts*. Br J Cancer, 2015. **112**(10): p. 1675-86.
41. Miyazaki, M., et al., *Oleoyl-CoA is the major de novo product of stearoyl-CoA desaturase 1 gene isoform and substrate for the biosynthesis of the Harderian gland 1-alkyl-2,3-diacylglycerol*. J Biol Chem, 2001. **276**(42): p. 39455-61.
42. Rios-Esteves, J. and M.D. Resh, *Stearoyl CoA desaturase is required to produce active, lipid-modified Wnt proteins*. Cell Rep, 2013. **4**(6): p. 1072-81.
43. Lounis, M.A., et al., *Oleate activates SREBP-1 signaling activity in SCD1-deficient hepatocytes*. Am J Physiol Endocrinol Metab, 2017. **313**(6): p. E710-E720.
44. Friedl, P. and K. Wolf, *Tumour-cell invasion and migration: diversity and escape mechanisms*. Nat Rev Cancer, 2003. **3**(5): p. 362-74.
45. Krakhmal, N.V., et al., *Cancer Invasion: Patterns and Mechanisms*. Acta Naturae, 2015. **7**(2): p. 17-28.
46. Friedl, P. and S. Alexander, *Cancer invasion and the microenvironment: plasticity and reciprocity*. Cell, 2011. **147**(5): p. 992-1009.
47. Miyazaki, M., et al., *The biosynthesis of hepatic cholesterol esters and triglycerides is impaired in mice with a disruption of the gene for stearoyl-CoA desaturase 1*. J Biol Chem, 2000. **275**(39): p. 30132-8.
48. Berzat, A. and A. Hall, *Cellular responses to extracellular guidance cues*. EMBO J, 2010. **29**(16): p. 2734-45.
49. Weiger, M.C., et al., *Real-time motion analysis reveals cell directionality as an indicator of breast cancer progression*. PLoS One, 2013. **8**(3): p. e58859.
50. Igal, R.A., *Stearoyl CoA desaturase-1: New insights into a central regulator of cancer metabolism*. Biochim Biophys Acta, 2016. **1861**(12 Pt A): p. 1865-1880.
51. Chen, Y., Y. Zheng, and D.A. Foster, *Phospholipase D confers rapamycin resistance in human breast cancer cells*. Oncogene, 2003. **22**(25): p. 3937-42.
52. Luyimbazi, D., et al., *Rapamycin regulates stearoyl CoA desaturase 1 expression in breast cancer*. Mol Cancer Ther, 2010. **9**(10): p. 2770-84.

53. Cazzolli, R., et al., *Phospholipid signalling through phospholipase D and phosphatidic acid*. IUBMB Life, 2006. **58**(8): p. 457-61.
54. Coomans de Brachene, A., et al., *PDGF-induced fibroblast growth requires monounsaturated fatty acid production by stearoyl-CoA desaturase*. FEBS Open Bio, 2017. **7**(3): p. 414-423.
55. Navarro-Tito, N., T. Robledo, and E.P. Salazar, *Arachidonic acid promotes FAK activation and migration in MDA-MB-231 breast cancer cells*. Exp Cell Res, 2008. **314**(18): p. 3340-55.

A**All breast cancer****B****Triple-negative breast cancer****Figure 1**

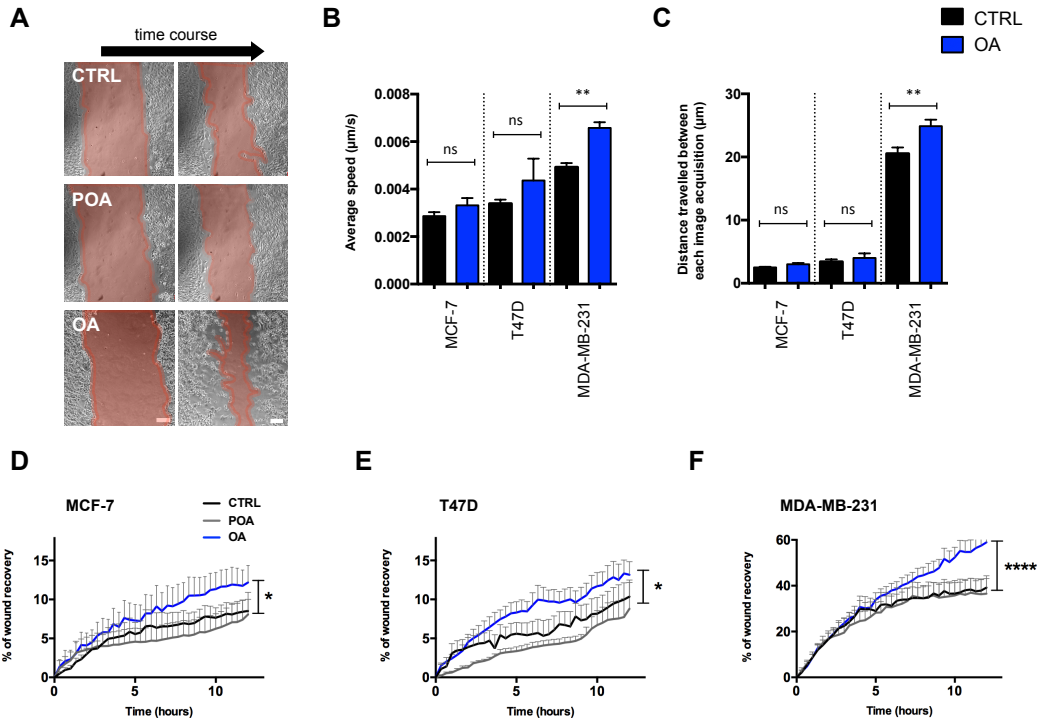
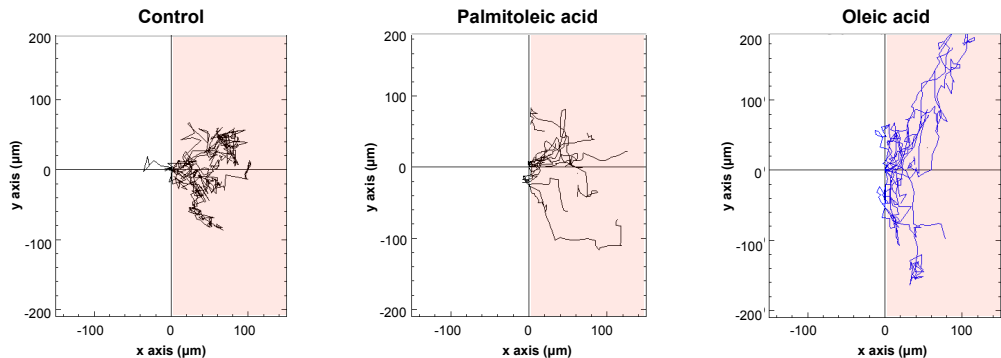
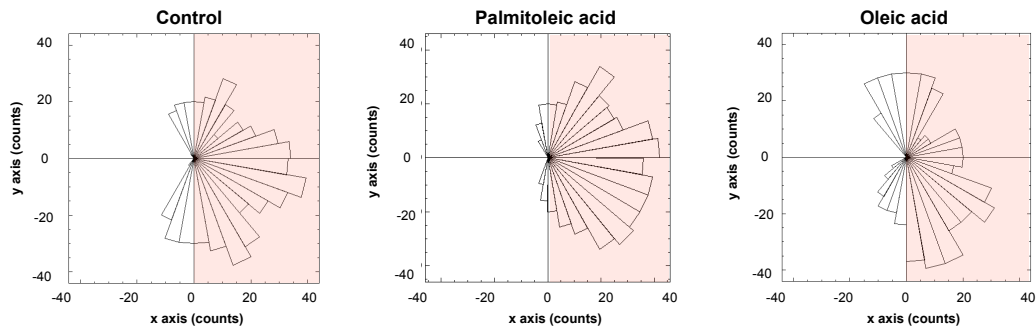


Figure 2

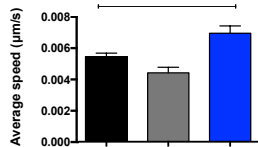
A Cell tracks



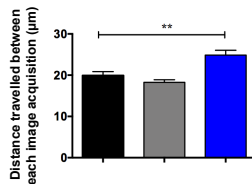
B Frequency of cell displacement orientation



C



D



E

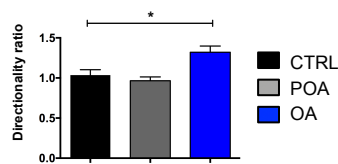


Figure 3

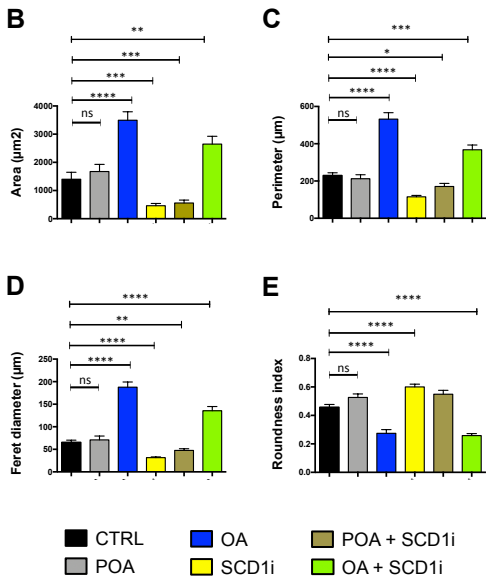
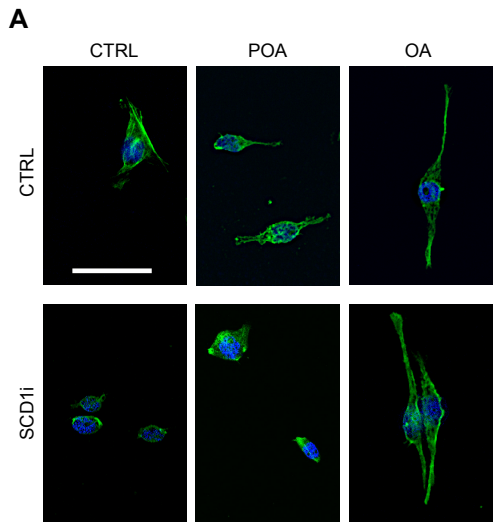


Figure 5

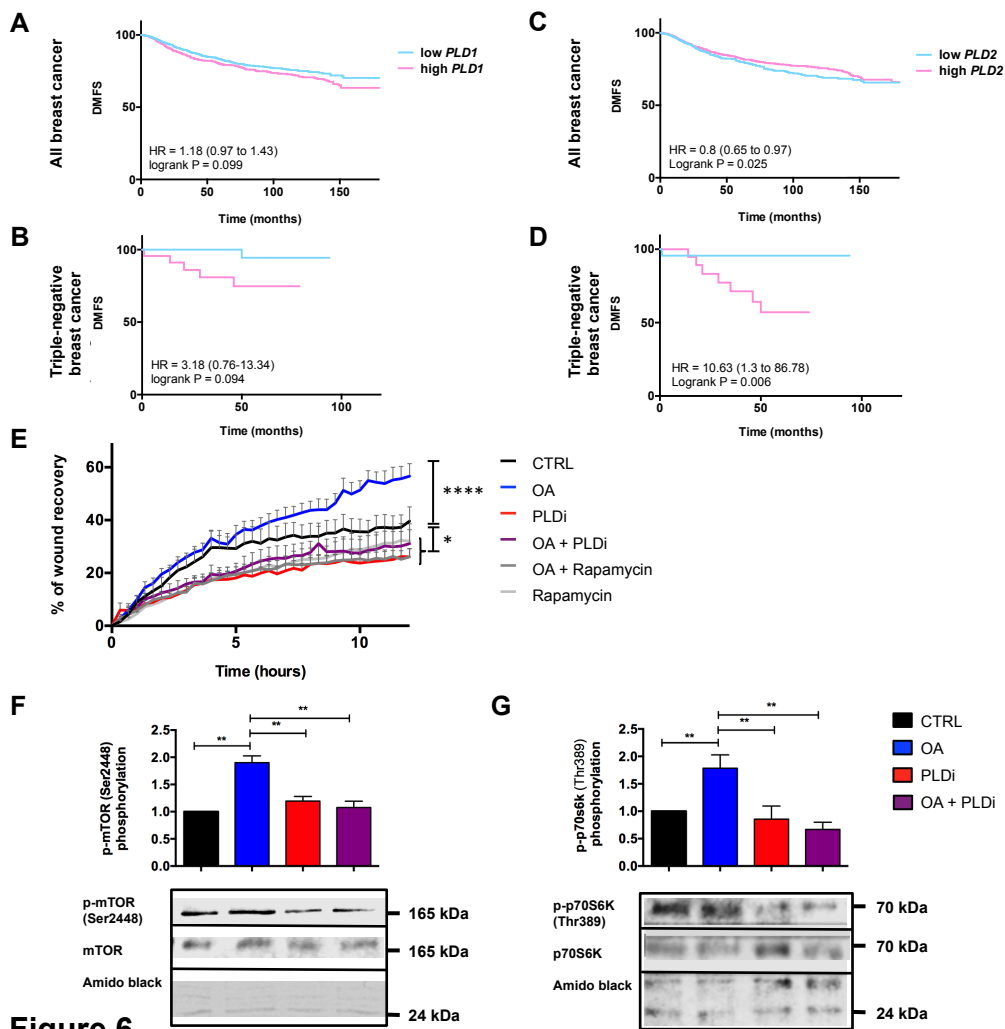
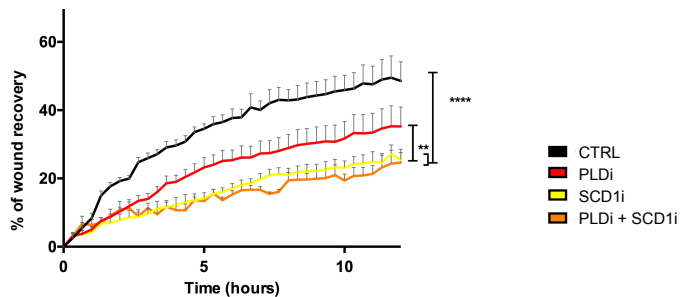
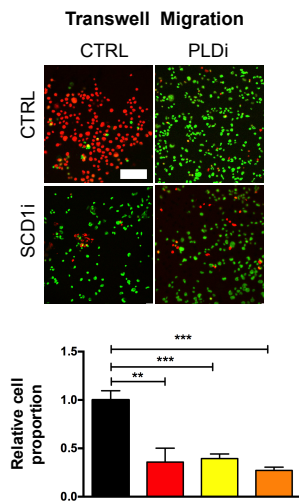
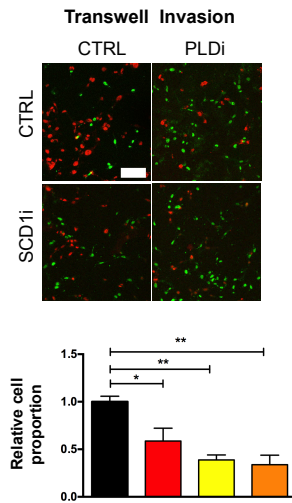
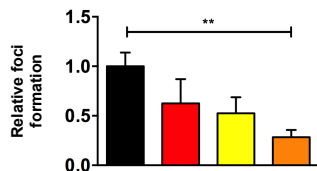
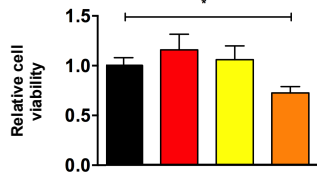


Figure 6

A**B****C****D****E****Figure 7**

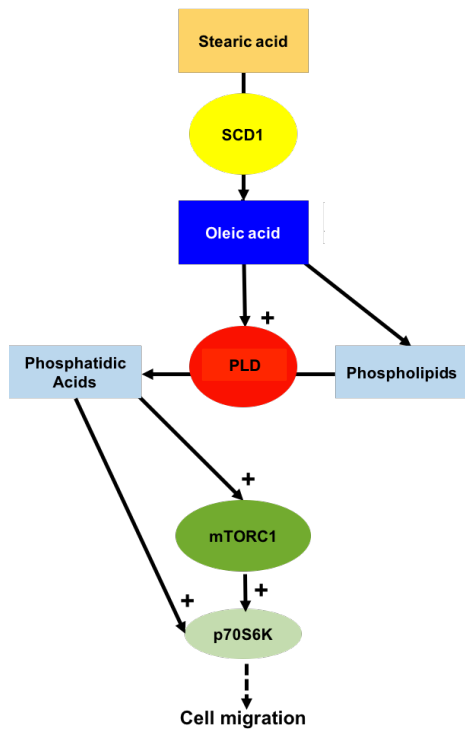
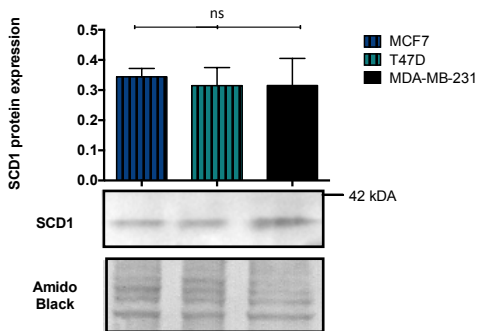


Figure 8



Supplementary Figure 1